MC/MO Study of the Solvent Effect on the Excitation Energies of the $(CH_3)_2NO$ Radical in Hydrogen-Bonding and Non-Hydrogen-Bonding Solvents

Toru Yagi, Kenji Morihashi, and Osamu Kikuchi*

Department of Chemistry, University of Tsukuba, Tsukuba 305-8571, Japan

Received: April 10, 2001; In Final Form: June 15, 2001

A combination of Monte Carlo (MC) simulation and ab initio molecular orbital (MO) calculation was applied to dimethyl nitroxide (DMNO) in H_2O, CH_3OH, CH_3CN, and $(CH_3)_2CO$ solutions, and the solvent effect on the electronic structure and $n-\pi^*$ and $\pi-\pi^*$ excitation energies was analyzed. The solution structures were generated by MC simulations, and the ROHF-SCI calculation with the MIDI-4 basis set was carried out for each solution structure. The electronic structure and excitation energies in the four solutions were obtained by averaging the 100 solution structures for each solution. Solvent effect was calculated by the point charge model and supermolecule model. In the point charge model, all solvent molecules were approximated by point charges at atomic nuclei, while in the supermolecule model the solute molecule and some of the solvent molecules were treated as a supermolecule surrounded by other solvent molecules approximated by point charges. The calculated $n-\pi^*$ excitation energy increased (blue shift) in the four solvents as compared to that in the gas phase. The magnitude of the solvent effect reflects the dielectric constant of the solvent. The calculated $E_{n-\pi^*}$ value in CH_3OH was larger than that in CH_3CN, whose dielectric constant is larger than that of CH_3OH. This is due to the hydrogen-bonding ability of CH_3OH and agrees well with experiment. The $\pi-\pi^*$ excitation energy was predicted to decrease in the four solvents, although the red shift was overestimated. The solvent effect was well elucidated by using the Mulliken charges of DMNO in the ground state and the excited states and the electrostatic potential generated by the solvent molecules.

I. Introduction

Nitroxide radicals are very popular radicals in various research areas.[1−24] ESR spectra of dimethyl nitroxide (DMNO), $(CH_3)_2NO$, have been observed in H_2O and $CHCl_3$;[2,3] the hyperfine coupling constant (hfcc) of the N atom (a_N) is larger in H_2O than in $CHCl_3$. Di-*tert*-butyl nitroxide (DTBN), $((CH_3)_3C)_2NO$, is a stable radical, and its a_N value has been determined in various solvents.[1,4,5,7−14] The a_N value of DTBN is larger in polar solvents.

The solvent effect on the excitation energies of nitroxide radicals has been reported since the mid-1960s.[4,14,25−28] For dialkyl nitroxide radicals,[4,14,26] the $n-\pi^*$ excitation energies were observed in many solvents and cover from 21 500 to 23 000 cm^{-1}. For cyclic nitroxide radicals,[25,27] the $n-\pi^*$ and $\pi-\pi^*$ excitation energies were observed in various solvents. The $n-\pi^*$ excitation energy shifts largely as in the case of the dialkyl nitroxide radicals. However, for the $\pi-\pi^*$ excitation energy, the shift by the solvent effect is small and does not show a clear tendency. The excitation energies of the H_2NO radical were calculated first by Kikuchi[6] and recently by Ricca et al.[16,17] The $\pi-\pi^*$ excitation energy was overestimated to some extent in these studies.

In many cases, the solvent effect on the electronic structure of the nitroxide radical was studied by ESR experiment.[2−4,14,25] Symons et al. showed a high correlation between the $n-\pi^*$ excitation energy and a_N and suggested that the solvent effects on these two quantities originated in the same cause.[14] In our previous theoretical works,[20−22] the hfcc's of the N atom of DMNO were evaluated by using the MC/MO method, and the difference in the hydrogen-bonding or non-hydrogen-bonding solvents was reproduced well. However, there have been no theoretical studies of the solvent effect on the excitation energies of DMNO.

In this paper, the MC/MO combined method was applied to calculate the $n-\pi^*$ and $\pi-\pi^*$ excitation energies of DMNO in four solvents: H_2O, CH_3OH, CH_3CN, and $(CH_3)_2CO$. The solution structures were generated by MC simulation, and the excitation energies were calculated by the ROHF-SCI/MIDI-4 method. The SCI method may not be sufficient to calculate quantitatively the excitation energies of free radicals. In this study, we were concerned with the effect of the solvent on the ground state and the SCI excited wave functions. The electronic structure of DMNO in these solutions and the solvent effect on the excitation energies were clarified.

II. Methods of Calculation

A. Monte Carlo Simulation. The C_{2v} molecular structure was assumed for DMNO and optimized by ROHF/MIDI-4d calculation in vacuo, while experimental geometries were adopted for H_2O, CH_3OH, CH_3CN, and $(CH_3)_2CO$.[29] For the H_2NO radical, a pyramidal structure has been calculated to be more stable than the planar one.[30,31] However, the energy difference between the planar structure and pyramidal one is very small in aqueous solution.[15] Moreover, the methyl groups in DMNO conjugate with the NO π group and the present assumption of the planar geometry of DMNO may be reasonable.

MC simulations for the H_2O, CH_3OH, CH_3CN, and $(CH_3)_2CO$ solutions were carried out for the NPT ensembles according to the standard Metropolis method.[32] Each solution included one DMNO molecule and 215 solvent molecules in a cubic cell, and the periodic boundary condition was employed. A cutoff

10.1021/jp0113230 CCC: $20.00
Published on Web 08/09/2001

length for the potential was half of an edge of the cubic cell. The system pressure was set at 1 atm and the temperature at 298 K. The Owicki−Scheraga−Jorgensen preferential sampling technique[33−35] was employed. Each simulation covered at least 2000K steps for equilibration, followed by additional 3000K steps for averaging. MC simulations were carried out using the SIMPLS program coded for the present purposes.

B. Point Charge Model and Supermolecule Model. After establishing equilibrium for the solution structure in the MC simulation, the solution structures were picked up and the solvent molecules were treated in two ways as described below. One is a point charge model and the other is a supermolecule model. In the point charge model, solvent molecules located inside the cutoff length from the solute molecule were represented by point charges; the magnitudes of the point charges were the same as those used in the potential functions for the MC simulation. In the supermolecule model, some of the solvent molecules close to the solute molecule were selected and treated explicitly as a supermolecule together with the solute molecule. Thus the ab initio MO calculation was carried out for the supermolecule including one DMNO and the selected solvent molecules which was surrounded by other solvent molecules approximated by point charges.

The H_2O molecules included in the supermolecule were selected in the order of the distance parameter, $\tilde{R}_{AB}$, defined between the sites of the solute and solvent molecules:

$$\tilde{R}_{AB} = \frac{R_{AB}}{r_A + r_B} \quad (1)$$

where r_A and r_B are van der Waals radii of sites A and B, respectively, and R_{AB} is the distance between these sites. In this selection, the H_2O molecules distribute around the DMNO uniformly.

C. Calculation of Excitation Energies. The following Hamiltonian was used for the MO calculation:

$$\hat{H} = \sum_k \left(-\frac{1}{2}\nabla_k^2 \right) + \sum_{k<l} \left(\frac{1}{r_{kl}} \right) - \sum_k \sum_A \left(\frac{Z_A}{r_{kA}} \right) - \sum_k \sum_s \left(\frac{q_s}{r_{ks}} \right) + \sum_A \sum_s \left(\frac{Z_A q_s}{r_{As}} \right) \quad (2)$$

where k and l are electrons and A is a nucleus. The first, second, and third terms of the right-hand side are the Hamiltonian of the electrons in a supermolecule and represent the kinetic energy of electrons, the electrostatic repulsion between two electrons, and the electrostatic attraction between an electron and a nucleus, respectively. The fourth and fifth terms are the electrostatic interactions between an electron and a point charge and between a nucleus and a point charge, respectively. These two terms represent the interaction between the supermolecule and the solvent molecules approximated by point charges. The electronic structure of the supermolecule surrounded by the point charges and the effect of the electrostatic and electron delocalization interaction were evaluated by using this Hamiltonian.

ROHF-SCI/MIDI-4 calculation was carried out to evaluate the $n-\pi^*$ and $\pi-\pi^*$ excited states of DMNO in the H_2O, CH_3OH, CH_3CN, and $(CH_3)_2CO$ solutions. In the present SCI calculation for the doublet states, four types of singly excited configurations[6] were considered, and all singly excited configurations between the occupied orbital except the core orbitals and the virtual orbital whose orbital energy is less than 2.00 hartree were included. The energies of the ground and excited states in each solution were calculated by averaging the energies of 100 solution structures. It is noted that the solution structures used in the CI calculation were in equilibrium with the ground state of DMNO, and vertical excitation energies were obtained.

MO calculations were carried out using our ABINIT and GUGACI programs on HPC Alpha workstations.

TABLE 1: Calculated Excitation Energies of DMNO in the Gas Phase (in cm^{-1})

method	$E_{n-\pi^*}$	$E_{\pi-\pi^*}$
ROHF-SCI	22 554	53 046
MCSCF/SOCI[a]	20 300	49 800
expt[b]	21 500	42 200

[a] Calculated values for H_2NO, ref 17. [b] Experimental values for DTBN in pentane, ref 26.

TABLE 2: The $n-\pi^*$ Excitation Energies (in cm^{-1}) of DMNO in Four Solvents Calculated by the Point Charge Model

	$E_{n-\pi^*}$	
solvent	ROHF-SCI	expt[a]
$(CH_3)_2CO$	23 398	22 026
CH_3CN	23 583	22 222
CH_3OH	23 828	22 831
H_2O	25 461	23 753

[a] Experimental values for DTBN, ref 14.

III. Results and Discussion

A. MC Simulation. The MC simulation was described in the previous paper.[21] It has been pointed out that hydrogen bonding is formed in H_2O and CH_3OH solution while it is not recognized in CH_3CN and $(CH_3)_2CO$ solutions. Since the MC simulations were carried out by using the potential functions for the ground state of DMNO, the solution structures selected are appropriate for the ground state DMNO. Thus, the relaxation of solvent structures was not allowed in the MO calculation of the excited states. The calculated excitation energies correspond to the vertical excitations about the electronic structure.

B. MO Calculation and Excitation Energy of DMNO. *1. Point Charge Model.*

Table 1 shows the calculated excitation energies of the DMNO radical in the gas phase. The MCSCF/SOCI calculation of H_2NO[17] and the experimental values for DTBN in pentane[26] are also shown. The present ROHF-SCI calculation reproduced well the experimental $n-\pi^*$ excitation energy. For the $\pi-\pi^*$ excitation energy, the ROHF-SCI result overestimated the experimental value by about 10 000 cm^{-1}.

The $n-\pi^*$ excitation energies ($E_{n-\pi^*}$) of DMNO calculated in the four solvents are listed in Table 2 and plotted in Figure 1 against the dielectric constant of the solvent. When all solvent molecules were represented by point charges located at each atomic nuclei, the $E_{n-\pi^*}$ value was increased by 2907, 1274, 1029, and 844 cm^{-1} in the H_2O, CH_3OH, CH_3CN, and $(CH_3)_2CO$ solutions, respectively, as compared with that in the gas phase. The $E_{n-\pi^*}$ value is the largest in the H_2O solution and is the smallest in the $(CH_3)_2CO$ solution. The $E_{n-\pi^*}$ value of DTBN has been observed in various solvents: it increases with increasing solvent dielectric constant, and it is larger in a hydrogen-bonding solvent than in a non-hydrogen-bonding solvent when two solvents have nearly equal magnitude dielectric constants. The calculated excitation energies in the four solutions agree well with these experimental facts for DTBN.[14]

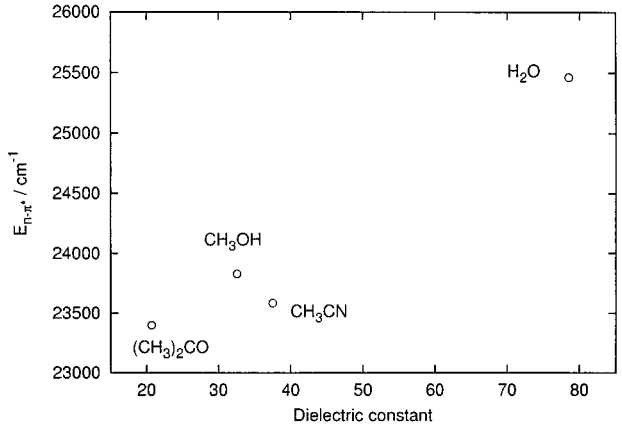

Figure 1. The $n-\pi^*$ excitation energies of DMNO in the four solvents calculated by the point charge model.

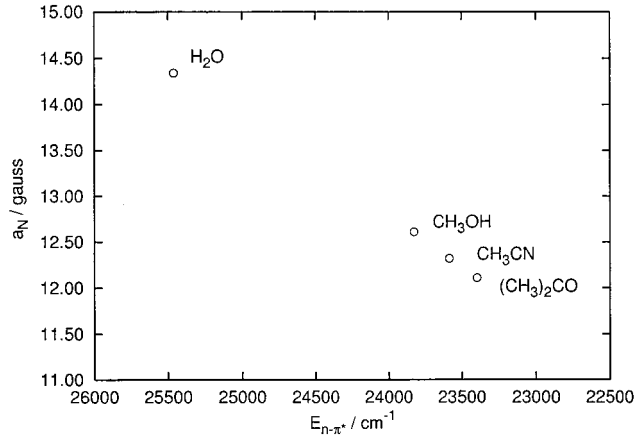

Figure 2. Correlation between the calculated $n-\pi^*$excitation energies and the hfcc of the N atom of DMNO. All solvent molecules were approximated by point charges.

As described below, about 75% of of the solvent effect is reproduced by the point charge model calculation. Thus, the solvent effect on $E_{n-\pi^*}$ is caused primarily by the electrostatic interaction between DMNO and the solvent. The point charge model also reproduced well that the $E_{n-\pi^*}$ value is larger in the hydrogen-bonding solvents than in the non-hydrogen-bonding solvents. Since the hydrogen-bonding solvent molecule has a specific orientation to the solute molecule, the resulting large electrostatic interaction polarizes the π N−O bond and increases the solute dipole moment. The electrostatic interaction between the solute and solvent molecules makes the ground state stabilize. This is why the $E_{n-\pi^*}$ value in the CH_3OH solution is larger than that in the more polar CH_3CN solution even in the point charge model calculations.

The hfcc of the N atom of DTBN also has been determined experimentally in various solvents.[12] The shifts of the hfcc value caused by four solvents show the same trend as that for the $E_{n-\pi^*}$ value. Symons et al. found experimentally a high correlation between the excitation energies and a_N values of DTBN in various solvents.[14] In Figure 2, the calculated $E_{n-\pi^*}$ excitation energies are plotted to the a_N values which were calculated in our previous work.[21] The MC/MO calculation reproduced well the correlation between the excitation energy and the a_N value.

Figure 3 shows the solvent dependence of three electronic states of DMNO. The ground state is stabilized in solution as compared with the gas phase. However, the stabilization of the $n-\pi^*$ state by solvent is smaller than the ground state.

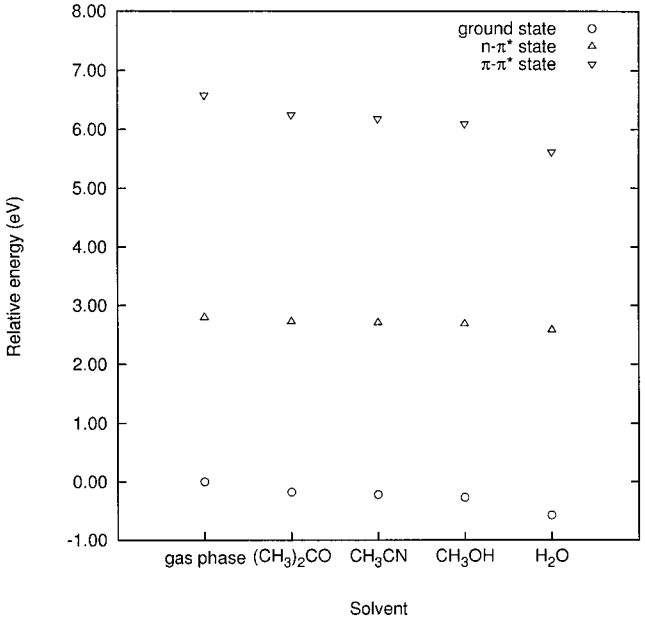

Figure 3. Solvent dependence of three electronic states of DMNO. The energies are relative values with respect to the energy of the ground state in the gas phase. All solvent molecules were approximated by point charges.

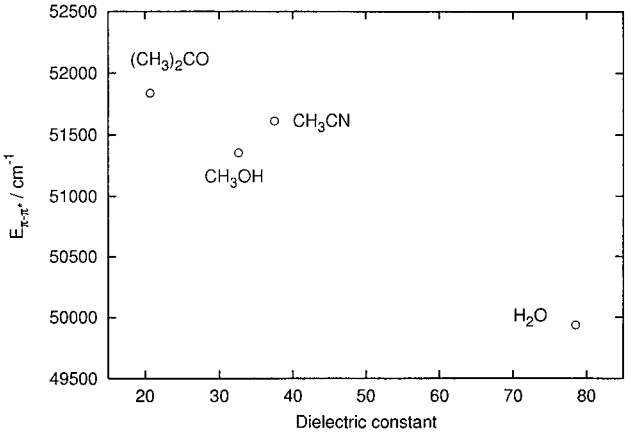

Figure 4. Correlation between the calculated $\pi-\pi^*$ excitation energy of DMNO and the dielectric constant of solvent.

TABLE 3: The $\pi-\pi^*$ Excitation Energies (in cm^{-1}) of DMNO in Four Solvents Calculated by the Point Charge Model

solvent	$E_{\pi-\pi^*}$ ROHF-SCI
$(CH_3)_2CO$	51 839
CH_3CN	51 611
CH_3OH	51 354
H_2O	49 936

Therefore, the $E_{n-\pi^*}$ value increases in solution and the increase is attributed mainly to the stabilization of the ground state.

The $\pi-\pi^*$ excitation energies ($E_{\pi-\pi^*}$) of DMNO calculated in the four solvents are listed in Table 3 and plotted in Figure 4 against the dielectric constant of the solvent. The $E_{\pi-\pi^*}$ value decreases in these solvents as compared with that in the gas phase. This means the $\pi-\pi^*$ state is stabilized by solvent more than the ground state. The magnitude of the decrease in $E_{\pi-\pi^*}$ is almost the same as that of the increase in the $n-\pi^*$ excitation energy. There are few experimental observations for the $\pi-\pi^*$ excitation energies of dialkyl nitroxide. In nitroxide radicals such as 2,2,6,6-tetramethylpiperidinyl-1-oxy (TEMPO), the solvent

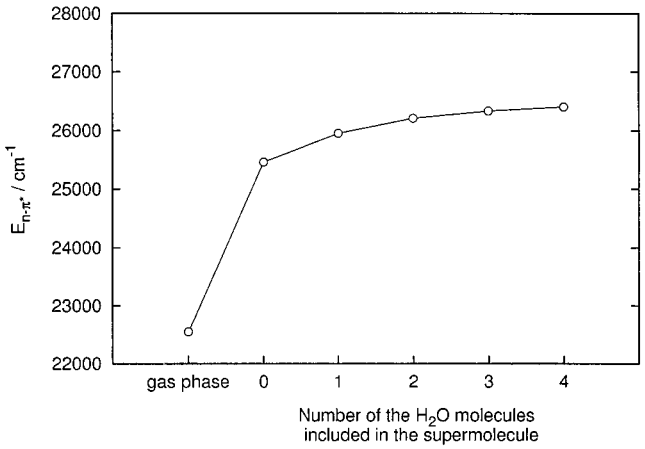

Figure 5. The $n-\pi^*$ excitation energies of DMNO in the H_2O solution calculated by the supermolecule model.

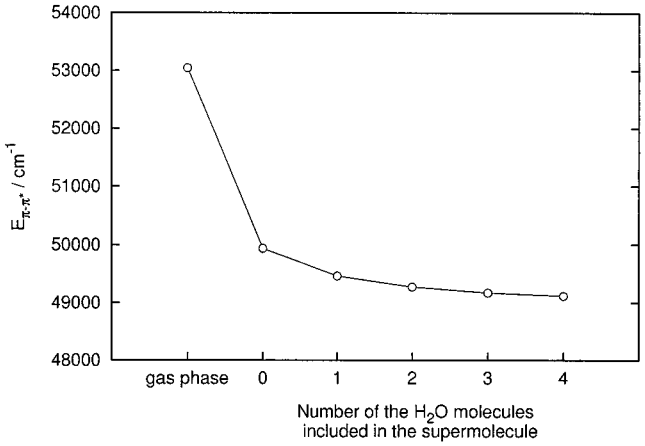

Figure 6. The $\pi-\pi^*$ excitation energies of DMNO in the H_2O solution calculated by the supermolecule model.

effect on the $\pi-\pi^*$ excitation energy is very small and no remarkable trends were observed in the solvent effect on the $\pi-\pi^*$ excitation energy.[25] The present result is contradictory to the experiment: the present calculation overestimated the stabilization of the $\pi-\pi^*$ excited state by solvent. This overestimation might be caused by inadequacy of the present SCI wave function to describe the solvent effect for the $\pi-\pi^*$ excited state.

2. Supermolecule Model in Aqueous Solution. Distribution of the H_2O molecules which are selected in the supermolecule calculation is similar to that reported in the previous paper.[21] Most H_2O molecules selected by the first selection in each solution structure are located near the O atom in DMNO. When the selection comes later, distribution of H_2O becomes uniform around DMNO.

Figures 5 and 6 show the calculated $E_{n-\pi^*}$ and $E_{\pi-\pi^*}$ values in H_2O, respectively, as a function of the number of water molecules included in the supermolecule. In the supermolecule model, n H_2O molecules ($n = 1-4$) were taken into account explicitly and an ab initio SCI calculation was applied to the DMNO$-n$H$_2$O supermolecule surrounded by point charges of other H_2O molecules. When the number of H_2O molecules that are included in the supermolecule is increased, the $E_{n-\pi}$* value increases while $E_{\pi-\pi}$* value decreases; they seem to converge at $n = 4$. This tendency is the same as that observed in the a_N values of DMNO.[21]

Figure 7 shows the charge of the three electronic states of DMNO as a function of the number of water molecules included

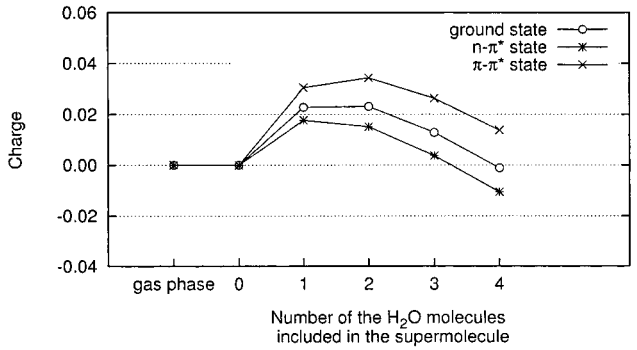

Figure 7. The charge of each electronic state of DMNO calculated by the supermolecule model.

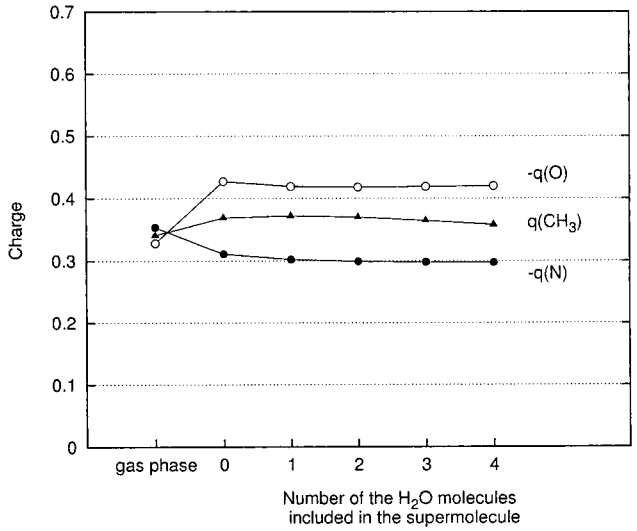

Figure 8. Mulliken charges at the O and N atoms and the methyl groups of DMNO in the ground state. The O and N atomic charges are multiplied by -1, and $q(CH_3)$ values are the averaged charges of two methyl groups.

in the supermolecule. The numbers on the ordinate indicate the number of electrons transferred from DMNO to the solvent. When one H_2O molecule was taken into account explicitly, appreciable electron transfer was recognized between DMNO and the H_2O molecule. The charge of DMNO is $+0.0228$, $+0.0177$, and $+0.0305$ in the ground state, the $n-\pi^*$ state, and the $\pi-\pi^*$ state, respectively; electron transfer occurs from DMNO to the H_2O molecule. The charge of the $n-\pi^*$ state is less positive compared to that of the ground state. By contrast, the charge of the $\pi-\pi^*$ state is more positive compared to that of the ground state. In the ground state, electron transfer occurs from the oxygen lone-pair electrons of DMNO to the H_2O molecule. In the $n-\pi^*$ state, the electron excites from the nonbonding orbital of the O atom to the π^* orbital which is spread over the N and O atoms. Therefore, the electron population around the O atom of DMNO is reduced and the electron transfer to the H_2O molecule is suppressed. In the $\pi-\pi^*$ state, the π-electron population is increased at the O atom, and the electron transfer is enhanced.

3. Electronic Structure and Solvent Effect. Figure 8 shows the Mulliken atomic charges in the ground state as a function of the number of water molecules included in the supermolecule. The charge distribution of the ground state is the same as in the previous paper.[21] The π-electron polarization in the N$-$O group is enhanced in water. In addition, electron transfer occurs in two directions: one is from DMNO to water around the O

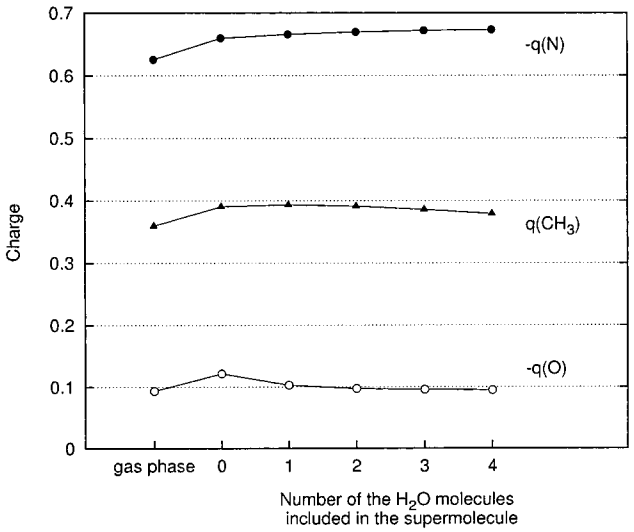

Figure 9. Mulliken charges at the O and N atoms and the methyl groups of DMNO in the $n-\pi^*$ state. The O and N atomic charges are multiplied by -1, and $q(CH_3)$ values are the averaged charges of two methyl groups.

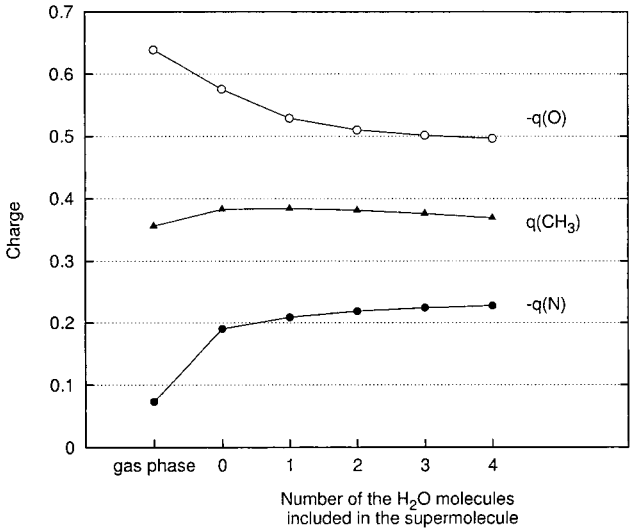

Figure 10. Mulliken charges at the O and N atoms and the methyl groups of DMNO in the $\pi-\pi^*$ state. The O and N atomic charges are multiplied by -1, and $q(CH_3)$ values are the averaged charges of two methyl groups.

atom in the N−O group and the other is from water to DMNO around the methyl groups.[21]

Figure 9 shows the Mulliken atomic charges in the $n-\pi^*$ excited state. The N and O atoms have negative charges. The magnitude of the negative charge of N is much larger than that in the ground state, while that of O is smaller than that in the ground state. This is due to the electron excitation from the nonbonding orbital of the O atom to the π^* orbital which is spread over the N and O atoms. When all solvent molecules were approximated by point charges, the charges of both the O and N atoms increased and large polarization of the N−O group, which was recognized in the ground state, was not observed in the $n-\pi^*$ state. The π system of DMNO has three π electrons, and in the $n-\pi^*$ state, the π and π^* orbitals are fully occupied and there are no polarized resonance structures. Since the π resonance does not exist, the polarization of the N−O group does not occur. Stabilization according to the electrostatic interaction with solvent is small in the $n-\pi^*$ excitation state. This is the reason why the $n-\pi^*$ state was little affected by solvation, while the ground state was stabilized largely as shown in Figure 3.

When one water molecule was taken into account explicitly in the supermolecule, the negative charge of O decreased in the $n-\pi^*$ excited state. This comes from the fact that the electron transfers from DMNO to water through the hydrogen bonding. When the second and third H_2O molecules were included explicitly in the supermolecule, the positive charges of the CH_3 groups decreased gradually. This is due to the reverse electron transfer from H_2O to DMNO through the CH_3 groups. The variation in the charge of DMNO also supports this electron transfer mechanism in aqueous solution. This variation resembles that of the ground state.

In the present supermolecule model, electron transfer occurs in two directions, from DMNO to H_2O through the N−O group and from H_2O to DMNO through the CH_3 groups. This seems very reasonable and suggests that BSSE does not cause any serious effects on the electronic structure of DMNO in the supermolecule calculation.

Figure 10 shows the Mulliken atomic charges in the $\pi-\pi^*$ excited state. In the $\pi-\pi^*$ state of an isolated DMNO, the negative charge of the O atom is larger and that of the N atom is smaller than the corresponding values as compared to those of the ground state. The $\pi-\pi^*$ excited state has the more polarized charge distribution than the ground state. When all water molecules were represented by point charges, the negative charges of the O atom decreased while that of the N atom increased. Thus, the polarization of the N−O bond is suppressed in aqueous solution. However, the dipole of this state is still larger than that of the ground state. This large polarization makes the $\pi-\pi^*$ excitation state stable. Therefore, the stabilization of the $\pi-\pi^*$ excitation state is larger than that in the ground state as in Figure 3; the $\pi-\pi^*$ excitation energy becomes smaller by solvation.

When one water molecule was taken into account explicitly in the supermolecule, the negative charge of the O atom decreased while the negative charge of the N atom increased in the $\pi-\pi^*$ excited state. The electron transfer occurs not only from DMNO to water through the hydrogen bonding but also from the O atom to the N atom through the π orbital. The dipole moment would be smaller than that obtained when all water molecules were represented by point charges.

When the number of H_2O molecules that were included in the supermolecule increased, the polarization of the N−O group decreased. When four H_2O molecules were included explicitly in the supermolecule, the polarization of the N−O group in the $\pi-\pi^*$ state was larger than that in the ground state. Therefore, the $\pi-\pi^*$ state of DMNO was stabilized more than the ground state by electrostatic interaction between DMNO and H_2O molecules and the $\pi-\pi^*$ excitation energy became small as compared to that in the gas phase.

4. Electrostatic Potential of DMNO and H_2O Molecules. Figure 11 shows the electrostatic potential (EP) around DMNO generated by the H_2O molecules. The solvent distribution was obtained on the average of 100 structures of the H_2O solution. The plane which the EP map is drawn on is perpendicular to the CCNO plane of DMNO and contains the N−O bond axis. When the N−O bond axis is put on the *z*-axis and the N atom on the origin, the *z*-coordinate of the O atom is 1.253 Å. The positive area of the EP is concentrated around the O atom of DMNO. The positive EP in this region is due to the H atom of H_2O which is in the hydrogen bonding with DMNO. In the vicinity of the N−O group, the EP due to the solvent H_2O increases monotonously along the *z*-axis. The electric field produced by such potential makes the N−O group polarize and

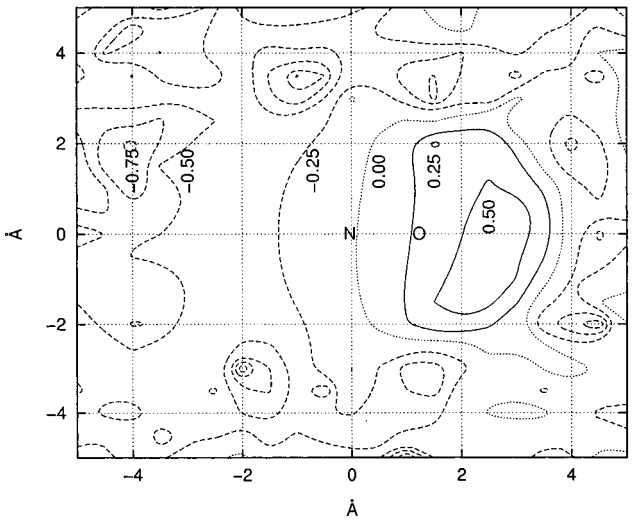

Figure 11. Electrostatic potential (EP) generated by solvent H_2O molecules (in hartrees). The EP is drawn on the plane which contains the N−O bond and is perpendicular to the CCNO plane of DMNO. The solid lines represent positive EP and the broken lines negative EP. The contour lines are drawn in steps of 0.25 hartree.

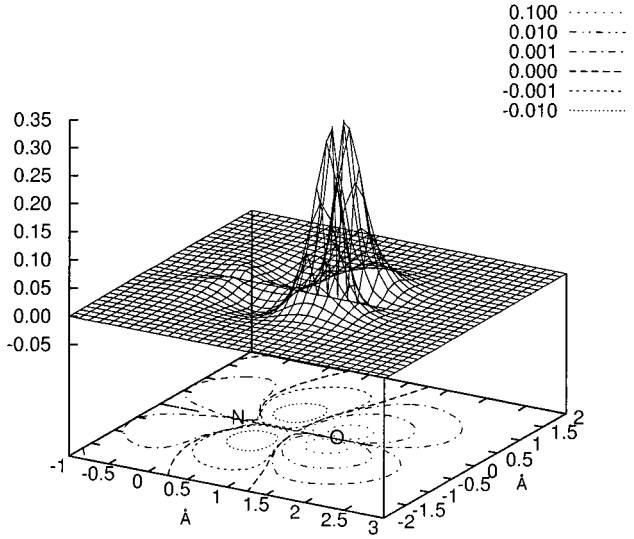

Figure 12. Difference of the electron density between the ground state and the $\pi-\pi^*$ excited state of DMNO in the gas phase. The plane contains the N−O bond and is perpendicular to the CCNO plane of DMNO.

the negative charge of the O atom increases. Actually, as shown in Figures 8 and 9, the polarization of the N−O group by solvent was enhanced in the ground and $n-\pi^*$ states. However, a reverse change was observed in the $\pi-\pi^*$ state.

Figure 12 shows the difference between the electron density of the ground state and the $\pi-\pi^*$ state in the plane defined in Figure 11. The ROHF wave function was used to calculate the electron density of the ground state, while the SCI wave function was used for the $\pi-\pi^*$ excitation state. When an electron is excited from the π orbital to the π^* orbital, the electron density decreases around the N atom and increases around the O atom. This is reflected also in the Mulliken population analysis in Figure 10.

Figure 13 shows the EP maps of DMNO in the ground state, $n-\pi^*$ state, and $\pi-\pi^*$ state on the plane defined in Figure 11. These maps were calculated by using the single Slater determinant wave function that corresponds to each excited state. The negative EP is very deep in the $\pi-\pi^*$ state as compared to those of the ground state and the $n-\pi^*$ state. This is due to

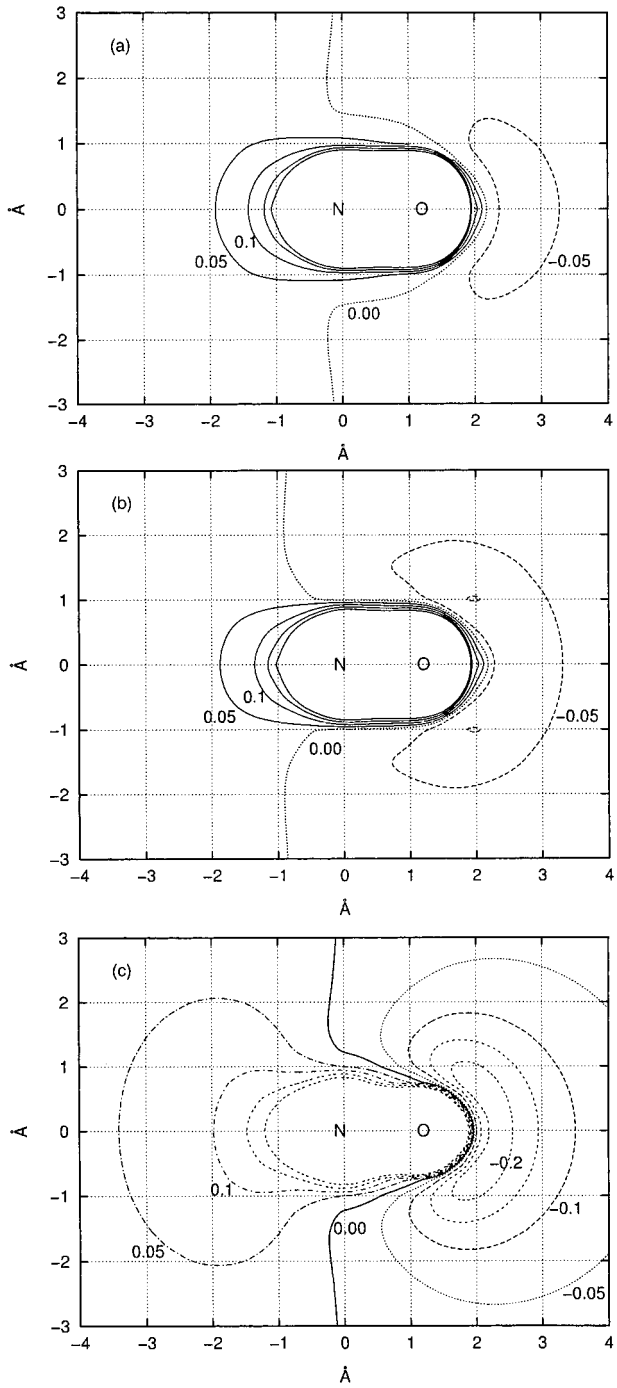

Figure 13. Electrostatic potential (EP) of (a) the ground state, (b) the $n-\pi^*$ state, and (c) the $\pi-\pi^*$ state of DMNO. The EP is drawn on the plane which contains the N−O bond and is perpendicular to the CCNO plane of DMNO. The solid lines represent positive EP and the broken lines negative EP. The contour lines are drawn in steps of 0.05 hartree.

the increase of the electron population around the O atom in the $\pi-\pi^*$ state that is shown in Figure 12. In the $\pi-\pi^*$ state, the electrostatic repulsion between the electron in the π^* orbital and the negative charge of the O atom of the H_2O which is in hydrogen bonding with the O atom of DMNO increases in the H_2O solution. The decrease of the population of the O atom of DMNO in Figure 10 is caused by this electrostatic repulsion.

IV. Conclusion

The excitation energies of DMNO in the H_2O, CH_3OH, CH_3CN, and $(CH_3)_2CO$ solutions were calculated by the MC/ROHF-

SCI/MIDI-4 combined method, and the solvent effect on the excitation energy of DMNO was elucidated. The calculated blue shift of the $n-\pi^*$ excitation in these solutions reflects the dielectric constant and the hydrogen-bonding ability of the solvent and agrees with the experimental trend observed for di-*tert*-butyl nitroxide in solutions. The experimentally observed correlation between the $n-\pi^*$ excitation energy and hyperfine coupling constant of nitrogen in DMNO was also reproduced well. The supermolecule model calculation in aqueous solution showed that about 25% of the solvent effect on the blue shift of the $n-\pi^*$ excitation energy was caused by the electron delocalization between DMNO and the H_2O molecules. In this respect, the present MC/MO combined method is superior to the continuum model and the QM/MM methods which do not allow electron delocalization between the solute and solvent molecules. The $\pi-\pi^*$ excitation energy was predicted to decrease in the four solvents as compared to that in the gas phase. However, the red shift of the $E_{\pi-\pi^*}$ value was overestimated. This is partly attributed to the SCI wave function in which only singly excited configurations are included.

References and Notes

(1) Lemaire, H.; Rassat, A. *J. Chim. Phys.* **1964**, *61*, 1580.
(2) Adams, J. Q.; Nicksic, S. W.; Thomas, J. R. *J. Chem. Phys.* **1966**, *45*, 654.
(3) Florin, R. E. *J. Chem. Phys.* **1967**, *47*, 345.
(4) Kawamura, T.; Matsunami, S.; Yonezawa, T. *Bull. Chem. Soc. Jpn.* **1967**, *40*, 1111.
(5) Forshult, S.; Lagercrantz, C.; Torssell, K. *Acta Chem. Scand.* **1969**, *23*, 522.
(6) Kikuchi, O. *Bull. Chem. Soc. Jpn.* **1969**, *42*, 47.
(7) Murata, Y.; Mataga, N. *Bull. Chem. Soc. Jpn.* **1971**, *44*, 354.
(8) Griffith, O. H.; Dehlinger, P. J.; Van, S. P. *J. Membr. Biol.* **1974**, *15*, 159.
(9) Knauer, B. R.; Napier, J. J. *J. Am. Chem. Soc.* **1976**, *98*, 4395.
(10) Atherton, N. M.; Manterfield, M. R.; Oral, B.; Zorlu, F. *J. Chem. Soc., Faraday Trans. 1* **1977**, *73*, 430.
(11) Kolling, O. W. *Anal. Chem.* **1977**, *49*, 591.
(12) Reddoch, A. H.; Konishi, S. *J. Chem. Phys.* **1979**, *70*, 2121.
(13) Janzen, E. G.; Coulter, G. A. *Tetrahedron Lett.* **1981**, *22*, 615.
(14) Symons, M. C. R.; Pena-Nu nez, A. S. *J. Chem. Soc., Faraday Trans. 1* **1985**, *81*, 2421.
(15) Takase, H.; Kikuchi, O. *Chem. Phys.* **1994**, *181*, 57.
(16) Ricca, A.; Hanus, M.; Ellinger, Y. *Chem. Phys. Lett.* **1995**, *232*, 54.
(17) Ricca, A.; Weber, J.; Hanus, M.; Ellinger, Y. *J. Chem. Phys.* **1995**, *103*, 274.
(18) Barone, V. *Chem. Phys. Lett.* **1996**, *262*, 201.
(19) Barone, V.; Bencini, A.; Cossi, M.; di Matteo, A.; Mattesini, M.; Totti, F. *J. Am. Chem. Soc.* **1998**, *120*, 7069.
(20) Yagi, T.; Takase, H.; Kikuchi, O. *Chem. Phys.* **1998**, *232*, 1.
(21) Yagi, T.; Kikuchi, O. *J. Phys. Chem. A* **1999**, *103*, 9132.
(22) Yagi, T.; Suzuki, T.; Morihashi, K.; Kikuchi, O. *J. Mol. Struct.* (*Theochem*) **2001**, *540*, 63.
(23) Improta, R.; di Matteo, A.; Barone, V. *Theor. Chem. Acc.* **2000**, *104*, 273.
(24) Zverev, V. V.; Levin, Ya. A. *Russ. J. Phys. Chem.* **2000**, *74*, 133.
(25) Briere, R.; Lemaire, H.; Rassat, A. *Bull. Soc. Chim. Fr.* **1965**, 3273.
(26) Anderson, D. R.; Koch, T. H. *Tetrahedron Lett.* **1977**, *35*, 3015.
(27) Mukerjee, P.; Ramachandran, C.; Pyter, R. A. *J. Phys. Chem.* **1982**, *86*, 3189.
(28) Reichardt, C. *Solvents and Solvent Effects in Organic Chemistry*, 2nd ed.; VCH: Weinheim, 1988.
(29) Harmony, M. D.; Laurie, V. W.; Kuczkowski, R. L.; Schwendeman, R. H.; Ramsay, D. A.; Lovas, F. J.; Lafferty, W. J.; Maki, A. G. *J. Phys. Chem. Ref. Data* **1983**, *79*, 926.
(30) Ellinger, Y.; Subra, R.; Rassat, A.; Douady, J.; Berthier, G. *J. Am. Chem. Soc.* **1975**, *97*, 476.
(31) Takase, H.; Kikuchi, O. *J. Phys. Chem.* **1994**, *98*, 5160.
(32) Metropolis, N.; Rosenbluth, A. W.; Rosenbluth, M. N.; Teller, A. H.; Teller, E. *J. Chem. Phys.* **1953**, *21*, 1087.
(33) Owicki, J. C.; Scheraga, H. A. *Chem. Phys. Lett.* **1977**, *47*, 600.
(34) Owicki, J. C. *ACS Symp. Ser.* **1978**, *86*, 159.
(35) Jorgensen, W. L.; Bigot, B.; Chandrasekhar, J. *J. Am. Chem. Soc.* **1982**, *104*, 4584.